E-Journal of Advanced Maintenance Vol.13 No.2 (2022) 1-13
Japan Society of Maintenology

Long-term stability mechanism for the effect with WJP and buffing residual stress improving treatments

Lina YU[1,*], Kazuyoshi SAIDA[1], Kazutoshi NISHIMOTO[1], Hideki ARAKI[1], Kazuki SUGITA[1], Masataka MIZUNO[1], and Naoki CHIGUSA[2]

[1] *Osaka University, 2-1 Yamadaoka, Suita, Osaka 565-0871, Japan*
[2] *The Kansai Electric Power Co., Inc., 8 Yokota, 13 Goichi, Mihama-cho, Mikata-gun, Fukui 919-1141, Japan*

ABSTRACT

The mechanism for long-term stability of the compressive stress in nickel-based alloy 600 components of the pressurized water reactor (PWR) plants introduced by water jet peening (WJP) and buffing stress improving treatments has been investigated in the present study. After thermal aging at the maximum actual operating temperature in PWR plants of 340 ℃ for 50 h, considerable hardness reduction was observed in WJP and buffing treated samples, but it was still much higher than that in solution heat-treated (ST) sample. However, after thermal aging at the higher temperature of 700 ℃ for 120 h, which should cause complete recrystallization, the hardness not only in the WJP treated sample but also in the buffing treated sample decreased to the level nearly equal to that of the ST sample. Furthermore, positron lifetime analysis has revealed that vacancies introduced by WJP and buffing treatments were mostly annihilated after thermal aging at the actual operating temperature, however considerable part of dislocations still stably remained. Based on these results, it has been elucidated that the long-term stability of the compressive residual stress in PWR components introduced by WJP and buffing stress improvement treatment can be attributed to the remained dislocations of relatively stable situation in the actual operating condition of PWR plants.

KEYWORDS

Long-term stability, WJP, Buffing, Hardness, Positron lifetime

ARTICLE INFORMATION

Article history:
Received 10 May 2021
Accepted 17 November 2021

1. Introduction

Stress Corrosion Cracking (SCC) is one of the significant aging degradation problems for the nickel-based alloy components in the primary reactor water environment in the PWR type of nuclear power plants. In general, SCC is a phenomenon that occurs with the superimposed three factors such as corrosive environment, sensitive material, and especially tensile residual stress due to welding. It is generally known that SCC can be prevented if any one of these factors is eliminated. For instance, in order to prevent SCC, reduction of tensile residual stress is effective, and various stress improvement methods to reduce the tensile residual stress have been proposed and used in practical operation, such as water jet peening (WJP), buffing and so on [1-3]. However, since PWRs are regularly operated at the temperature of about 300 ℃, occasionally at the maximum operating temperature of about 340 ℃. It has been concerned that during the PWR practical operation, the introduced compressive residual stress by these methods might be relaxed [4]. Therefore, in order to ensure the safety of the nuclear power plants from SCC, it should be very important to clarify the stress relaxation behavior introduced by the stress improving methods in such high temperature environment as in practical operation.

In the previous researches [5,6], it has been elucidated that the residual stress relaxation is related to the hardness reduction behavior. Based on this fact, the mechanism of the initial relaxation of the compressive stress introduced by the stress improving treatments at the actual PWR operating temperature has been investigated by the authors [7]. However, the mechanism of long-term stability of the compressive stress in the high temperature environment during the PWR practical operation is not clear yet, although an assumption has been proposed by the authors [7]. Therefore, in order to

* Corresponding author, E-mail: yulina@mapse.osaka-u.ac.jp

clarify the mechanism for long-term stability, the stress relaxation behavior of compressive stress introduced by WJP and buffing treatments during the thermal aging not only at the actual PWR operating temperature but also at the completely recrystallizing temperature has been studied in the present study. For this purpose, the hardness analysis, the electron back scattered diffraction (EBSD) crystal orientation analysis and the positron annihilation lifetime spectroscopy (PALS) analysis in the specimens with and without thermal aging have been conducted. Based on the obtained results, long-term stability mechanism of compressive residual stress introduced by WJP and buffing stress improving treatments during the practical plant operation has been discussed.

2. Materials and methods

The nickel-based 600 alloy with dimension 100 mm × 50 mm × 10 mm was used as work material in the present study, with the chemical composition shown in Table 1. WJP and buffing stress improving treatments were conducted on the sample surfaces without pre-mechanical grinding. In WJP treatment, the nozzle of WJP was set to pass vertically through the sample center, and the flow rate of water injection was 48 l/min. The buffing treatment was performed in the longitudinal direction using the same condition as the actual application to PWR plants.

The specimens for analysis were cut in the shape of 10 mm × 10 mm × 10 mm from the above samples by using the electrical discharge machining method, which can minimize the additional effect on the strain. The thermal aging was performed by using an electric furnace with the heating rate of 30 K/s followed by water quenching. In order to examine the completely recrystallizing conditions for WJP and buffing processed samples, the thermal aging temperatures were varied from 650 ℃ to 700 ℃, with the various holding time from 30 h to 120 h. For comparison, the thermal aging in the actual PWR operation environment was also carried out at 340 ℃ for 50 h. Here, 340 ℃ is approximately same as the actual maximum operating temperature of PWRs.

Vickers micro hardness measurement was performed the cross section of the polished specimens with a load of 245 mN and a dwell time of 15 s. The hardness distribution perpendicular to the processed surface was measured from the depth of 10 μm near the processed surface to the depth of 0.1 mm. The average of 7 measurements excluding the maximum and the minimum values was used in the present study.

The changes in crystal orientation near the processed surface of WJP and buffing treated specimens were investigated by the crystal orientation analysis using EBSD. Prior to observation, the samples were polished and electrolytically etched using the solution of 20 % methanol in sulfuric acid at room temperature with current density of 1.92 A/cm^2. The inverse pole figure (IPF) map, kernel average mis-orientation (KAM) map, grain orientation spread (GOS) map, and grain reference orientation deviation (GROD) map were obtained in the present study.

Positron annihilation lifetime spectroscopy (PALS) was used to quantitatively characterize the lattice defects in the specimens. PALS is capable to directly determine the free-volume defects at the atomic level and nanoscales, such as vacancies and dislocations. PALS can measure the elapsed time between the implantation of the positron into the material and the emission of annihilation radiation. Positron has a positive charge, so if there is no void or defect, it will disappear at the interstitial position away from the nucleus. When void or defect exists in the material, it is trapped and then pair-annihilated with the surrounding electron. Therefore, the positron lifetime is inversely proportional to the probability for electron to meet positron. Furthermore, as the lattice defect density increases, the proportion of positrons trapped at the defect position increases, resulting in the extension of the positron lifetime [8-11].

The positron lifetime was analyzed by PALS. The results were used to investigate quantitatively the lattice defects introduced by WJP and buffing treatments before and after thermal aging. Positron lifetime was measured using a digital oscilloscope system, yielding a time resolution of 187 ps, with photomultiplier tubes mounted with BaF_2 scintillators. The positron lifetime spectra were obtained at the coincidence count rate of 120 counts/s with a total number of (1-3) × 10^6 coincidence counts. The positron lifetime measurement was conducted in the room temperature, and the positron lifetime spectra were analyzed using the RESOLUTION [12] and POSITRONFIT extended [13] programs.

Table 1 Chemical composition (mass%) of alloy 600.

C	Si	Mn	S	Cu	Cr	Fe	Ni
0.001	0.19	0.49	0.001	0.01	15.5	7.97	Bal.

3. Recrystallizing condition for WJP stress improving treated specimens

In general, the recrystallizing condition of materials varies due to the strain introduced with the degree of plastic deformation. Therefore, recrystallizing condition in stress improving treated materials will also vary depending on the method of the stress improving treatment.

In order to examine the completely recrystallizing condition for WJP treated samples, the thermal aging was performed at the temperatures from 650 ℃ to 700 ℃, with the holding time varied from 30 h to 120 h. The hardness distribution perpendicular to the processed surface of the samples processed by WJP stress improving treatment after different thermal aging conditions was shown in Fig. 1, together with the result before thermal aging for comparison. The dashed line in the figure represents the hardness data (170 HV) of the ST sample. Before thermal aging, hardness increase was observed near the peened surface, which is due to the impact of cavitation on the surface. After thermal aging, the hardness of samples for all measured conditions has remarkably decreased to the level nearly equal to that of the ST sample. It can be also found that there is no significant difference in the hardness of the specimens when the thermal aging temperature was changed from 650 ℃ to 700 ℃ with varying the holding time from 30 h to 120 h. It suggests that recrystallization has occurred in all of these thermal aging conditions.

To examine the completely recrystallizing condition, EBSD crystal orientation analysis was also performed on the cross section of the sample under the thermal aging conditions of 650 ℃ for 30 h and 700 ℃ for 120 h. The results are illustrated in Fig. 2 by comparison with that before thermal aging. The upper part of each map shows the processed surface of the samples. According to the KAM, GOS, and GROD maps before thermal aging, some strain which seems to be introduced by WJP is observed near the peened surface. While after the thermal aging at 650 ℃ for 30 h, the residual strain was also recognized near the surface. However, after the thermal aging at the higher temperature of 700 ℃ for longer holding time of 120 h, significant strain relaxation was observed near the surface. In addition, some small grains were found to appear near the processed surface as shown in the IPF map of Fig. 2. It indicates that the recrystallization phenomenon has completed in the WJP treated samples with the thermal aging at 700 ℃ for 120 h.

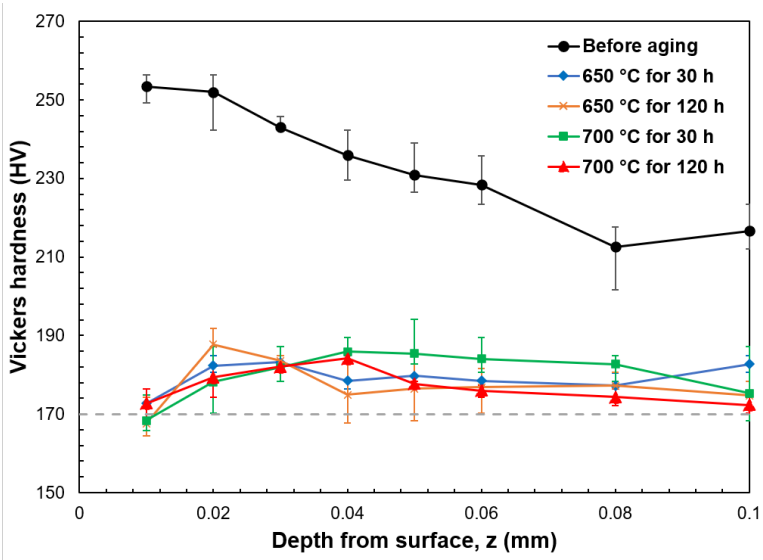

Fig. 1 Comparison of depth distribution of hardness in WJP treated samples with and without thermal aging at different thermal aging conditions.

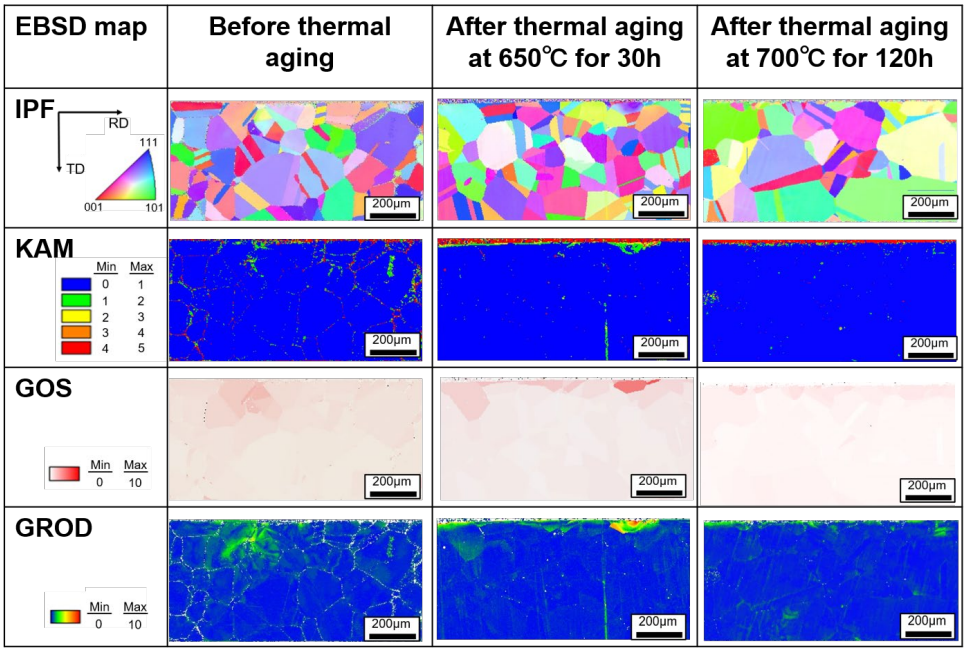

Fig. 2 Comparison of crystal orientation maps in WJP treated samples with and without thermal aging at different thermal aging conditions.

4. Recrystallizing condition for buffing stress improving treated specimens

For the buffing treated samples, the hardness distribution before and after thermal aging is illustrated Fig. 3. The dashed line in the figure represents the hardness in the ST sample. As presented in Fig. 3, the hardness after buffing stress improving treatment has increased mainly near the processed surface and gradually decreased from the processed surface to the inside of the specimen. In contrast, the hardness after thermal aging has decreased almost to the level close to that of the ST sample for each aging condition. Moreover, no significant difference was observed in hardness of the aged samples when the thermal aging temperature being varied from 650 ℃ to 700 ℃ with the holding time changed from 30 h to 120 h. It indicates that the recrystallization seems to be completed with each thermal aging condition for buffing treated samples.

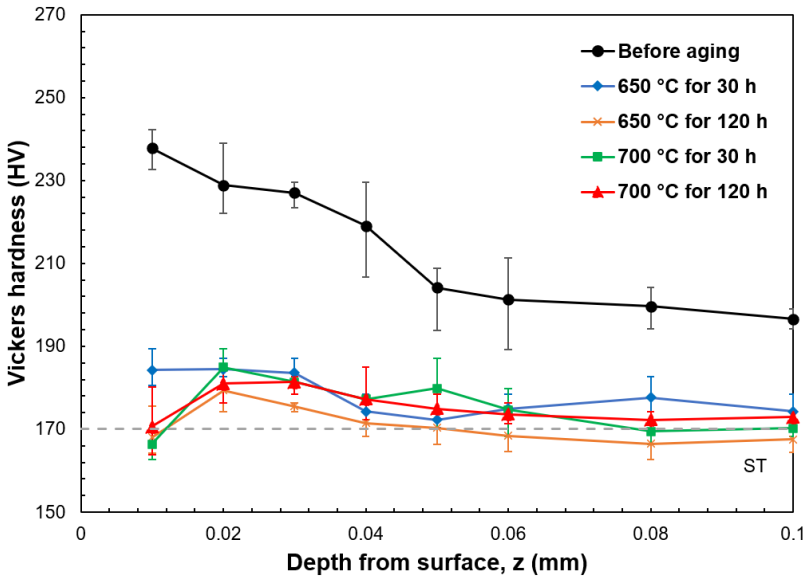

Fig. 3 Depth distribution of hardness in buffing treated samples with and without thermal aging at different thermal aging conditions.

In order to confirm the condition to complete recrystallization for buffing treated samples, EBSD crystal orientation analysis was also performed for the samples heat-treated with the conditions of 650 ℃ for 30 h and 700 ℃ for 120 h. The results are indicated in Fig. 4 together with the results before thermal aging. According to KAM, GOS, and GROD maps after thermal aging at 650 ℃ for 30 h, the residual strain can be also recognized near the processed surface. On the other hand, after thermal aging at the higher temperature of 700 ℃ for the longer holding time of 120 h, the considerable strain relaxation can be observed near the surface. In addition, the IPF map indicates that some small grains have formed near the processed surface. These results suggest that for the buffing treated samples, the recrystallization phenomenon has completed with the thermal aging at 700 ℃ for 120 h.

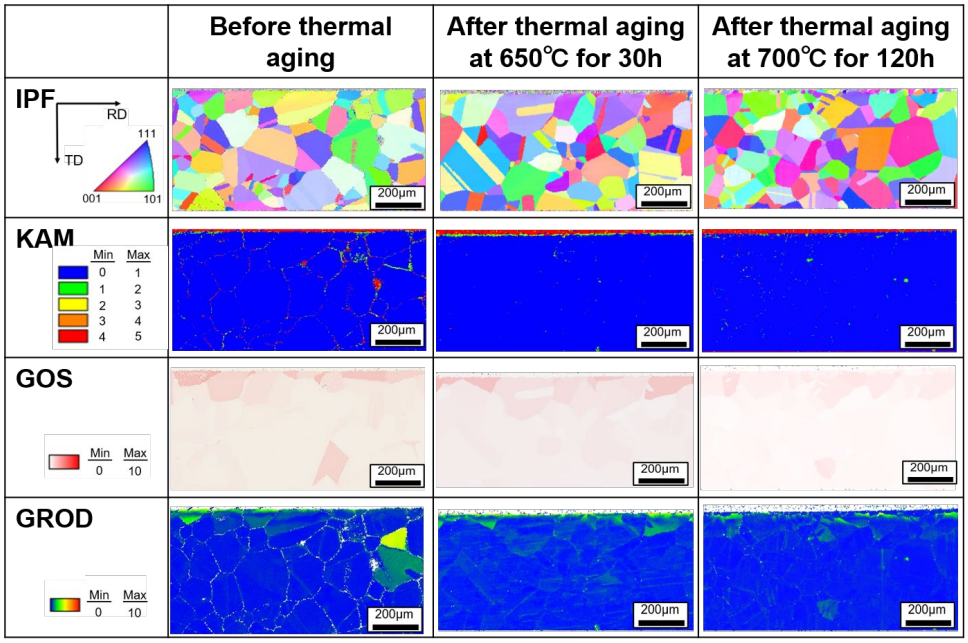

Fig. 4 Comparison of crystal orientation maps in buffing treated samples with and without thermal aging at different thermal aging conditions.

5. Comparison of residual stress relaxation behavior after thermal aging at the actual operating temperature and the completely recrystallizing temperature

5.1 Hardness comparison after thermal aging at the actual operating temperature and the completely recrystallizing temperature

The hardness distribution for the WJP treated samples after thermal aging to complete recrystallization was compared with the results of those aged at the actual operating temperature, as shown in Fig. 5. Here, the thermal aging at the maximum actual operating temperature of PWRs of 340 ℃ for 50 h was used for comparison. It can be found that after thermal aging at the maximum actual operating temperature of 340 ℃ for 50 h, the hardness significantly reduced, but still much higher than that of the ST sample. However, after thermal aging at the completely recrystallizing temperature of 700 ℃ for 120 h, the hardness has remarkably decreased to nearly equal to the result of the ST sample. It indicates that some strain near the processed surface introduced by WJP stress improving treatment partly remained even after thermal aging at the maximum actual operating temperature of 340 ℃ for a long time. However, after thermal aging at the completely recrystallizing temperature of 700 ℃ for 120 h, the introduced strain has almost relaxed because of the complete recrystallization phenomenon.

Similarly, the hardness distribution of the buffing treated samples after complete recrystallization thermal aging was also compared with the result of the specimen aged at the actual operating temperature, as shown in Fig. 6. Compared with the hardness before thermal aging, the hardness of

buffing treated sample after thermal aging at the maximum actual operating temperature of 340 ℃ for 50 h considerably reduced, but it was still much higher than that of the ST sample. However, after thermal aging at the higher completely recrystallizing temperature of 700 ℃ for 120 h, the hardness has completely decreased to the level of nearly equal to the ST sample. It follows that some strain near the processed surface introduced by buffing stress improving treatment has partly remained even after thermal aging at the maximum actual PWR operating temperature for a long time. However, after thermal aging at the completely recrystallizing temperature of 700 ℃ for 120 h, the introduced strain has almost relaxed due to completion of recrystallization.

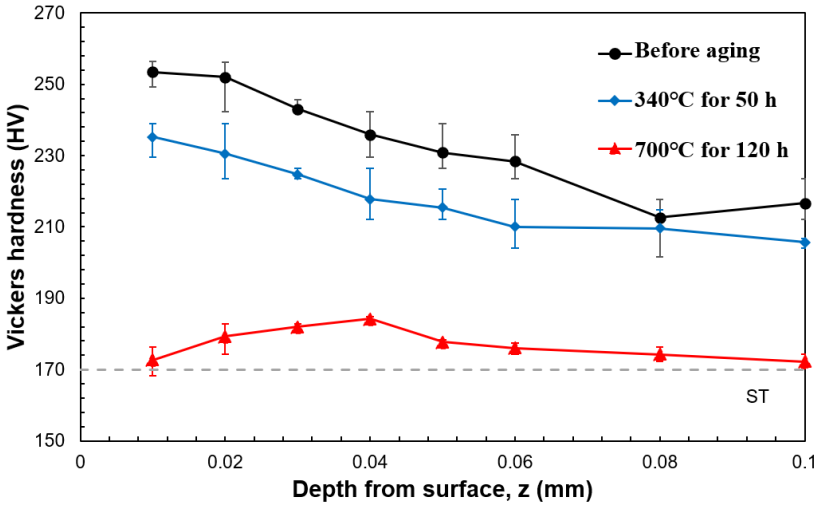

Fig. 5 Depth distribution of hardness in WJP treated samples with and without thermal aging at different temperatures.

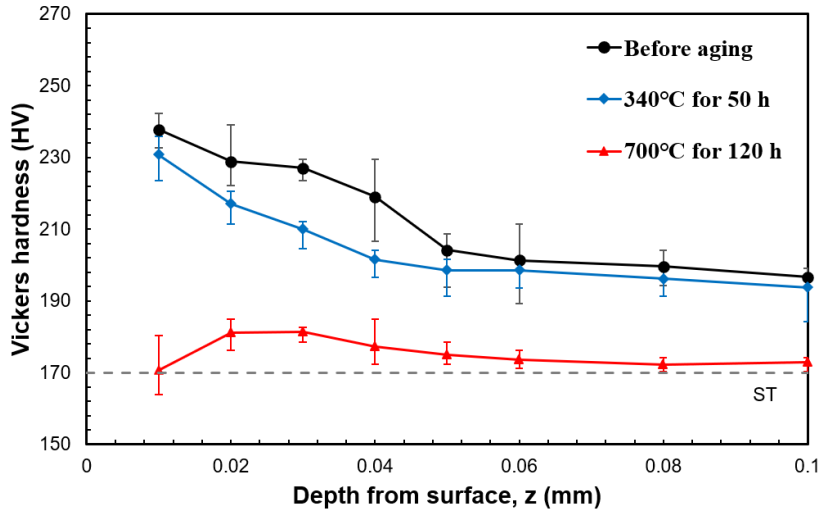

Fig. 6 Depth distribution of hardness in buffing treated samples with and without thermal aging at different temperatures.

5.2 Comparison of positron lifetime in the specimens aged at the actual operating temperature and the completely recrystallizing temperature

In order to examine the effect of recrystallization treatment on the internal defects in the WJP and buffing treated specimens, PALS was used to investigate the positron lifetimes in the material, which enables to evaluate the lattice defects quantitatively. After subtracting the source correction, the positron lifetime spectra were evaluated by one-component or two-component analysis to determine the mean positron lifetime. Fig. 7 exhibits the mean positron lifetimes in the WJP and buffing treated specimens after the thermal aging at the completely recrystallizing temperature, together with the

result at the actual PWR operating temperature [7] for comparison. The typical error of the mean positron lifetime in present study was ± 0.3 ps.

As shown in Fig. 7, a positron lifetime of 113.8 ps is observed in the ST sample, which is similar to the results determined in the defect-free constituent pure metals [14] (Ni: 108 ps, Fe: 110 ps, and Mn: 109 ps). It indicates that the obtained positron lifetime is the same as that in the ST sample in a free state. After the stress improving treatment, positron lifetimes of 183.7 ps and 166.5 ps were observed in WJP and buffing treated samples respectively, which were longer than that in the ST sample. This indicates that a large amount of lattice defects have been introduced by WJP and buffing treatments [7]. Furthermore, the positron lifetime of 183.7 ps in WJP treated sample was longer than that in buffing treated sample (166.5 ps), indicating that more lattice defects have been introduced by WJP treatment. While after thermal aging at the maximum actual operating temperature of 340 ℃ for 50 h, the mean positron lifetimes in WJP and buffing treated samples have reduced to 151.3 ps and 138.5 ps respectively, which are still much longer than that in the ST sample. It follows that even after thermal aging at the maximum actual operating temperature of 340 ℃ for 50 h, some lattice defects still partly remained. However, after the thermal aging at the completely recrystallizing temperature of 700 ℃, the positron lifetimes in both WJP and buffing treated samples have significantly reduced to 113.3 ps and 114.1 ps respectively, which are nearly equal to that in the ST sample. It indicates that the lattice defects introduced by WJP and buffing treatments have been annihilated completely, because of the recrystallization during the thermal aging at 700 ℃ for 120 h.

In order to evaluate the fraction and the amount of dislocation and vacancy defects in the WJP and buffing treated samples before and after thermal aging at the temperature to cause complete recrystallization, multi-component analysis of the spectra obtained by positron annihilation lifetime spectroscopy was performed by using the following equation (1).

$$N(t) = \sum_{i=1}^{n} \frac{I_i}{\tau_i} \exp\left(-\frac{t}{\tau_i}\right) \tag{1}$$

Here, *N(t)* is the counting rate, *I* is relative intensity, τ is positron lifetime, *n* is the component, and *t* is time.

Three-component analysis was used to evaluate the ratio and the amount of dislocation and vacancy defects, using the following equations (2)-(3).

$$C_d = \frac{1/\tau_f - 1/\tau_d + I_v\,(1/\tau_d - 1/\tau_v)}{1 - I_d - I_v} \times \frac{I_d}{\mu_d} \tag{2}$$

$$C_v = \frac{1/\tau_f - 1/\tau_v + I_d\,(1/\tau_v - 1/\tau_d)}{1 - I_v - I_d} \times \frac{I_v}{\mu_v} \tag{3}$$

Here, *C* is defect concentration, *I* is relative intensity, τ is positron lifetime, μ is trapping coefficient, *f* is free positron, *d* is dislocation, and *v* is vacancy. τ_f is the lifetime of free positrons, and the value of pure Ni alloy is 104 ps, and the trapping coefficients used in this study are shown as follows:

$\mu_d = 1.2\times10^{-4}\ m^2s^{-1}$, $\mu_v = 2.2\times10^{15}\ s^{-1}$.

Fig. 8 exhibits the dislocation density of the samples processed by WJP and buffing treatments before and after the thermal aging at the completely recrystallizing temperature, together with the result at the actual operating temperature for comparison. As shown in Fig. 8, the dislocation density in both WJP and buffing treated samples have decreased remarkably after the thermal aging at the maximum actual operating temperature of 340 ℃ for 50 h, while it is much higher than that in the ST sample. However, after the thermal aging at the higher completely recrystallizing temperature of 700 ℃ for 120 h, the dislocation density in both WJP and buffing treated samples have decreased nearly equal to that in the ST sample. It follows that the dislocation remained even after the thermal aging at the actual maximum operating temperature of 340 ℃ for 50 h has been annihilated completely after the thermal aging at the higher temperature of 700 ℃ for 120 h due to recrystallization.

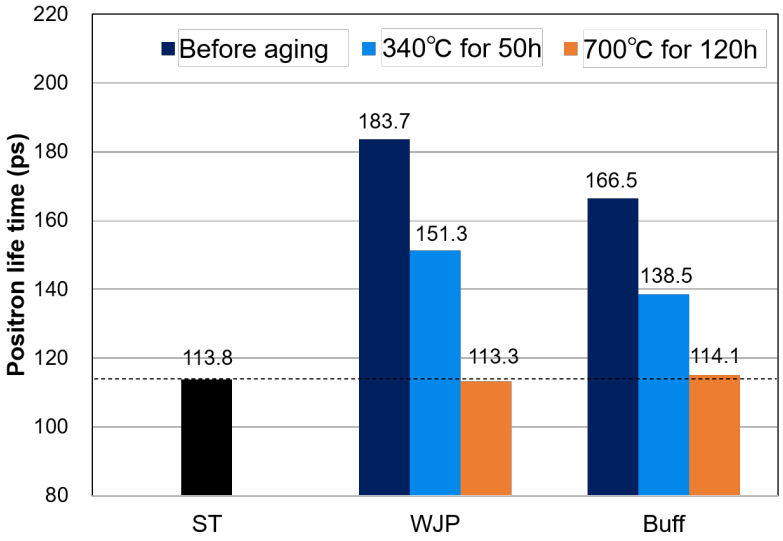

Fig. 7 Comparison of positron lifetime with and without thermal aging at different temperatures.

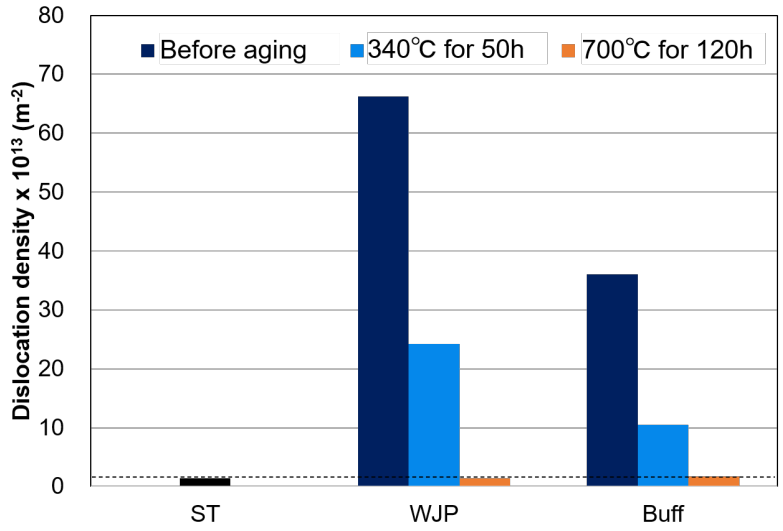

Fig. 8 Comparison of dislocation density with and without thermal aging at different temperatures.

The measured amounts of dislocations and vacancies in WJP and buffing treated specimens before and after thermal aging at the completely recrystallizing temperature are summarized in Table 2. The detailed relative intensity and lifetime of the lattice defects in WJP and buffing treated specimens are respectively presented in Fig. 9 and Fig. 10.

As shown in Table 2, after thermal aging, the amounts of both dislocations and vacancies have remarkably decreased in both WJP and buffing treated specimens. Especially such tendency is more dominant for the vacancies in both samples. In contrast, the dislocations have partly remained even after the thermal aging at the maximum actual PWR operating temperature of 340 ℃ for 50 h. The partially remained dislocations after the thermal aging at the actual PWR operating temperature have been significantly annihilated after the thermal aging at the completely recrystallizing temperature of 700 ℃ for 120 h in WJP and buffing treated specimens. On the other hand, larger amounts of both dislocations and vacancies are observed in WJP treated specimen than that in buffing treated specimen. It suggests that more lattice defects have been introduced by WJP treatment, especially for the vacancies. The reason for the less amount of vacancies in buffing treated specimen is considered due to the fact that some of the introduced vacancies have been annihilated on-site because of the increased temperature during the buffing process [6].

Furthermore, as shown in Fig. 9, the fractions of both dislocations and vacancies in the WJP treated specimen before thermal aging are both 49%, while after the thermal aging at the actual PWR

operating temperature, the fraction of dislocations has changed to 89%, and the fraction of vacancies has reduced to 2%. This fact suggests that almost all of the vacancies have been annihilated during thermal aging at the actual PWR operating temperature, while the dislocations partially remained. However, when the thermal aging was performed at the completely recrystallizing temperature of 700 ℃ which is much higher than the actual PWR operating temperature, the fraction of dislocations has reduced from 89% to 35%, and the vacancies have been mostly annihilated. These results are also consistent with the dislocations and vacancies measurements shown in Table 2. It indicates that the dislocations that remained partially after the thermal aging at the actual operating temperature have been mostly annihilated due to recrystallization with thermal aging at 700 ℃.

In addition, as illustrated in Fig. 10, the fraction of dislocations in the buffing treated specimen before thermal aging is about 81%, which is higher than that in the WJP treated specimen. However, the total amounts of both dislocations and vacancies are lower than that of the WJP treated specimen, as shown in Table 2. After the thermal aging at the actual PWR operating temperature, the fraction of vacancies has decreased from 13% to about 0%, indicating that almost all of the vacancies seem to be annihilated, but about one third of the dislocations still seem to remain. However, after the thermal aging at the completely recrystallizing temperature, the fraction of dislocations in the buffing treated specimen has decreased from 81% to 40%, which is almost the same amount of dislocations as in the ST sample. It follows that the partially remained dislocations after the thermal aging at the actual PWR operating temperature have been significantly annihilated after the thermal aging at the completely recrystallizing temperature, for both WJP and buffing treated samples.

Table 2 Comparison of dislocation density and vacancy concentration with and without thermal aging at different temperatures.

Condition		Dislocation density (m^{-2})	Vacancy concentration (ppm)
WJP	Before aging	6.63×10^{14}	37.0
	After aging at 340 ℃ for 50 h	2.42×10^{14}	0.32
	After aging at 700 ℃ for 120 h	1.37×10^{13}	0.00
Buff	Before aging	3.60×10^{14}	3.20
	After aging at 340 ℃ for 50 h	1.05×10^{14}	0.00
	After aging at 700 ℃ for 120 h	1.71×10^{13}	0.00
ST		1.42×10^{13}	0.00

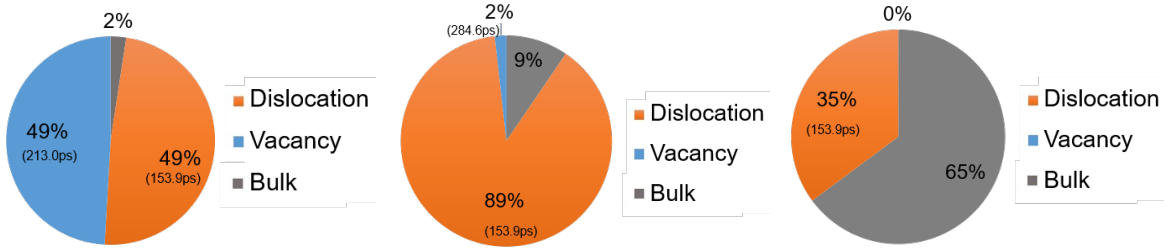

(a) before aging (b) after aging at 340 ℃ for 50 h (c) after aging at 700 ℃ for 120 h

Fig. 9 Relative intensity and lifetime of lattice defects in WJP treated samples with and without thermal aging at different temperatures.

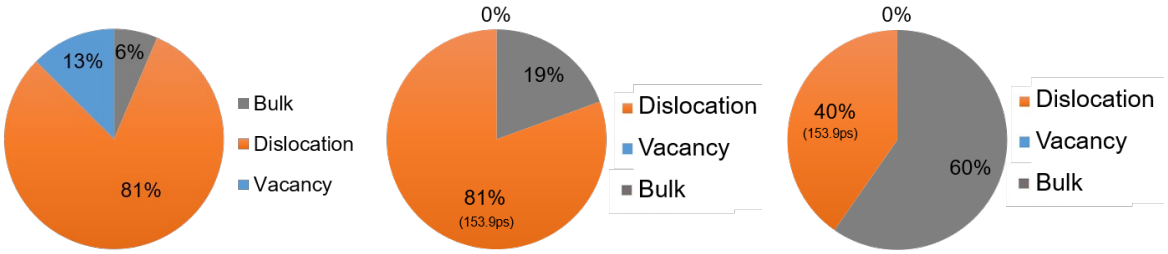

(a) before aging (b) after aging at 340 ℃ for 50 h (c) after aging at 700 ℃ for 120 h

Fig. 10 Relative intensity and lifetime of lattice defects in buffing treated samples with and without thermal aging at different temperatures.

6. Mechanism for long-term stability of residual stress introduced by WJP and buffing stress improving treatments

As mentioned above, the increased hardness near the surface in the sample caused by WJP and buffing stress improving treatments has significantly reduced after thermal aging at the maximum actual PWR operating temperature of 340 ℃ for 50 h, but still much higher than that in the ST sample. However, after the thermal aging at the higher completely recrystallizing temperature of 700 ℃ for 120 h, the hardness has so decreased to the level nearly equal to that of the ST sample, not only for WJP treated sample but also for the buffing treated sample. In the previous researches [5,6], it has been clarified that the residual stress relaxation behavior is related to the hardness reduction behavior. Therefore, it is considered that the WJP and buffing treated specimens show the similar residual stress relaxation behavior to the above mentioned hardness change.

In the present study, higher KAM, GOS, and GROD values are observed near the processed surface in both WJP and buffing treated specimens by EBSD analysis. However, after the thermal aging at the completely recrystallizing temperature, not only the hardness has decreased to the level nearly equal to that of the ST specimen, but also the strain near the processed surface has significantly relaxed, together with occurrence of some small grains near the processed surface. It suggests that the strain introduced by WJP and buffing treatments has been annihilated completely after thermal aging at the higher completely recrystallizing temperature, due to recrystallization.

It is well known that such miss-orientation information obtained by EBSD as KAM, GOS, and GROD is closely related to micro-deformation in the material, which is also reflected as dislocation density [15,16]. As mentioned above, the information obtained with KAM, GOS, and GROD indicates that micro-deformation near the processed surface remained in operation at the actual PWR operating temperature have been annihilated after the thermal aging at the higher completely recrystallizing temperature. This fact was also supported by the positron lifetime measurements in these materials. Positron lifetime analysis revealed that most of vacancies and some dislocations introduced with the micro-deformation by WJP and buffing treatments were annihilated during the initial stage of thermal aging at the actual PWR operating temperature, while the rest of the introduced dislocations remained stably even after long-term thermal aging at the actual PWR operating temperature. When the thermal aging temperature was such higher than the actual PWR operating temperature as enough to cause recrystallization phenomenon, the stably remained dislocations would be annihilated because of completion of recrystallization, as schematically illustrated in Fig. 11.

In addition, it is well understood that the activation energy Q has different values depending on the rate-determining mechanism. Regarding the activation energy of pure Ni and Ni-based alloys, Wuttig et al. has obtained a result of 154.3 kJ / mol as the activation energy of dislocation diffusion in pure Ni [17]. Furthermore, Wycisk et al. has reported that the activation energy for the movement of a single vacancy was 119.6 kJ / mol in pure Ni [18]. The lower activation energy for the vacancy movement suggests that the annihilation of vacancies is more easily to occur than the dislocation diffusion during thermal aging. This explains above mentioned phenomenon that during the thermal aging at the actual PWR operating temperature, almost all of the vacancies seem to be annihilated but the dislocations still seem to partially remain.

On the other hand, the activation energy Q of about 120 kJ / mol was obtained in the kinetic analysis of hardness reduction near the actual PWR operating temperature in both WJP and Buffing

treated samples [7]. The obtained activation energy Q was confirmed almost the same as the activation energy for vacancy movement and dislocation diffusion in pure Ni. It proves that the hardness reduction behavior during the thermal aging at the actual PWR operating temperature is also caused by the movement of vacancies, the diffusion or rearrangement of dislocations, and the consequent annihilation. According to the relationship between the hardness reduction behavior and the stress relaxation behavior, it can be concluded that the stress relaxation and long-term stability of the compressive stress in the actual PWR operation is also caused by the movement of vacancies and the diffusion or rearrangement of dislocations.

In the previous researches [3-7], it has been reported that the compressive stress introduced by the stress improvement method has relaxed partially in the early stage of thermal aging, and the rest remained stably during the long-term actual PWR operation. These results indicate that at actual PWR operating temperature, some of the introduced stresses have been relaxed in the early stage of thermal aging, while the other parts remain stably in the subsequent process of thermal aging. According to the results obtained in the present study, it is clear that the relaxation and the residual part of the compressive stress are closely related to the annihilation behavior of lattice defects. Namely as schematically illustrated in Fig.12, in the initial stage of thermal aging at the actual PWR operating temperature, most of vacancies and some of dislocations introduced by the residual stress improvement treatments have been annihilated after short period of thermal aging. As the thermal aging at the actual PWR operating temperature proceeds further, some parts of the dislocations are not annihilated but re-arranged, and then remain in relatively stable situation.

On the basis of the results, it has been elucidated that the long-term stability of the compressive stress in PWR components introduced by WJP and buffing stress improving treatments can be attributed to the remained dislocations of relatively stable situation in the actual operating temperature environment of PWR plants.

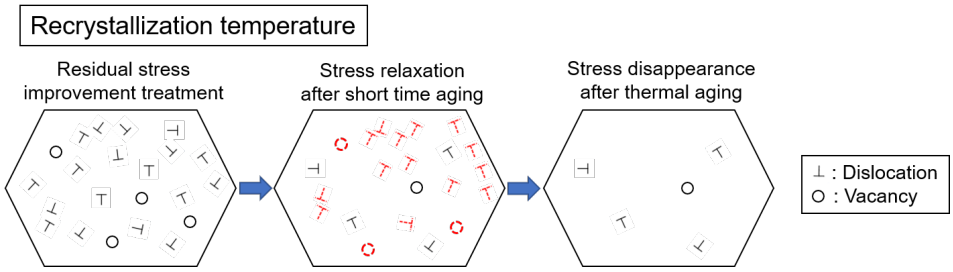

Fig. 11 Mechanism for residual stress relaxation during thermal aging at completely recrystallizing temperature.

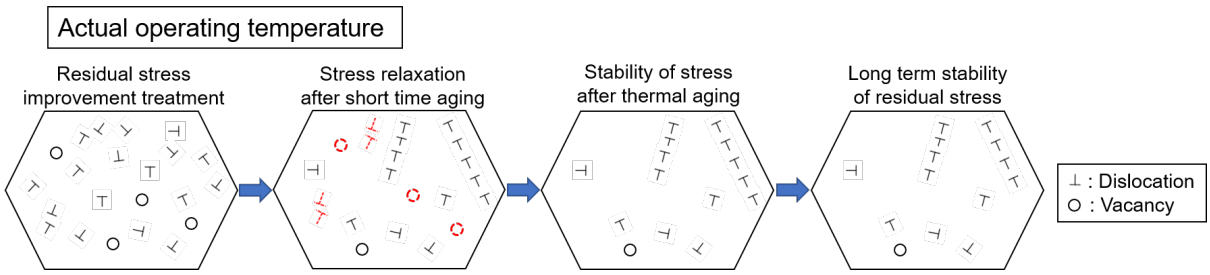

Fig. 12 Mechanism for residual stress relaxation and long-term stability of stress during thermal aging at actual operating temperature.

7. Conclusions

In order to elucidate the mechanism for long-term stability with WJP and buffing stress improving treatments at the actual PWR operating temperature, the stress relaxation behavior of the compressive stress in Alloy 600 components of the PWR plant during thermal aging has been studied in the present study. Based on the results, the long-term stability mechanism for compressive stress introduced by WJP and buffing treatments at the actual PWR operating temperature has been discussed. Main results obtained in the present study are as follows.

(1) According to hardness measurement and EBSD crystal orientation analysis, it has been clarified that recrystallization completely occurs during the thermal aging at 700 ℃ for 120 h in both WJP and buffing treated specimens.
(2) After thermal aging at the maximum actual PWR operating temperature, considerable hardness reduction was observed in WJP and buffing treated samples, but it was still much higher than that in solution treated sample. However, after thermal aging at the completely recrystallizing temperature, the hardness not only in the WJP treated sample but also in the buffing treated sample has decreased to the level nearly equal to that of the solution treated sample.
(3) Positron annihilation lifetime spectroscopy analysis has revealed that the dislocations remained stable at the actual PWR operating temperature have been significantly annihilated after the thermal aging at the completely recrystallizing temperature, for both the WJP treated sample and the buffing treated sample.
(4) It has been elucidated that the long-term stability of the compressive stress in PWR components introduced by WJP and buffing stress improving treatments can be attributed to the remained dislocations of relatively stable situation in the actual operating temperature environment of PWR plants.

Acknowledgment

The authors would like to gratefully acknowledge the assistance of Mr. Ikumi ASAI master of graduate school of engineering, Osaka University, Japan.

References

[1] S. Nishikawa, Y. Horii, K. Ikeuchi: “Stress Corrosion Cracking Morphology of Shielded Metal Arc Weld Metals for Alloy 600 in High Temperature Pressurized Pure Water”, Quarterly Journal of the Japan Welding Society, Vol. 27, pp. 67–72 (2009).
[2] D. Y. Ju, B. Han: “Investigation of water cavitation peening-induced microstructures in the near-surface layer of pure titanium”, Journal of Materials Processing Technology, Vol. 209, pp. 4789-4794 (2009).
[3] K. Okimura, T. Ohta, T. Konno, M. Narita, M. Toyoda: “Reliability of Water Jet Peening as Residual Stress Improvement Method for Alloy 600 PWSCC Mitigation”, Proceeding of the 16th International Conference on Nuclear Engineering, Vol. 1, pp. 565-570 (2008).
[4] R. Sumiya, D. Saito, I. Chida, Y. Yoshioka, K. Ishibashi, D. Kobayashi, A. Ito, M. Miyabe, M. Achiwa, K. Kishimoto: “Evaluation on Relaxation Behaviors of Compressive Residual Stress of Peened Ni-Base Superalloy Alloy 706 Test Specimens after Thermal Aging Treatment”, Journal of the society of materials science, Japan, Vol. 65, pp. 199-206 (2016).
[5] L. Yu, K. Saida, K. Nishimoto, N. Chigusa: “Relaxation behavior of residual stress generated by water jet peening under operation temperature environment - Evaluation for long term stability of residual stress improving treatment on Ni base alloy (report 1) –”, Maintenology, Vol. 18, pp. 91-98 (2019).
[6] L. Yu, K. Saida, K. Nishimoto, N. Chigusa: “Kinetic analysis on the long term stability of the effect obtained by various residual stress improvement methods - Evaluation for long term stability of residual stress improving treatment on Ni base alloy (report 2) –”, Maintenology, Vol. 18, pp. 99-106 (2019).
[7] L. Yu, K. Saida, H. Araki, K. Sugita, M. Mizuno, K. Nishimoto, N. Chigusa: “Mechanism for stress relaxation behavior of the residual stress improving treatments with water jet peening and buffing”, Materials Science & Engineering A, Vol. 796, 140221 (2020).
[8] Y. C. Jean: “Positron annihilation spectroscopy for chemical analysis: A novel probe for microstructural analysis of polymers”, Microchemical Journal, Vol. 42, pp. 72-102 (1990).
[9] B. Li, V. Krsjak, J. Degmova, Z. Wang, T. Shen, H. Li, S. Sojak, V. Slugen, A. Kawasuso: “Positron annihilation spectroscopy study of vacancy-type defects in He implanted polycrystalline α-SiC”, Journal of Nuclear Materials, Vol. 535, pp. 152-180 (2020).
[10] K. Saarinen, P. Hautojärvi, C. Corbe: “Chapter 5 Positron Annihilation Spectroscopy of Defects in Semiconductors”, Semiconductors and Semimetals, Vol. 51, pp. 209-285 (1998).
[11] R. W. Siegel: “Positron annihilation spectroscopy”, Ann. Rev. Mater. Sci., Vol. 10, pp. 393-425 (1980).
[12] P. Kirkegaard, M. Eldrup, O. E. ogensen and N. J. Pedersen: “Program system for analysing positron lifetime spectra and angular correlation curves”, Computer Physics Communications, Vol. 23, pp. 307-335 (1981).
[13] P. Kirkegaard and M. Eldrup: “POSITRONFIT extended: A new version of a grogram for analysing positron lifetime spectra”, Computer Physics Communications, Vol. 7, pp. 401-409 (1974).

[14] J M Campillo Robles, E. Ogando and F. Plazaola:" Positron lifetime calculation for the elements of the periodic table" J. Phys.: Condens. Matter, Vol. 19, 176222 (2007).
[15] K. Nomura, K. Kubushiro, Y. Sakakibara, S. Takahashi, H. Yoshizawa: "Effect of grain size on plastic strain analysis by EBSD for austenitic stainless steels with tensile strain at 650℃", Journal of the society of materials science, Japan, Vol. 61, pp. 371-376 (2012).
[16] K. Kubushiro, Y. Sakakibara, T. Ohtani: "Greep strain analysis of austenitic stainless steel by SEM/EBSD", Journal of the society of materials science, Japan, Vol. 64, pp. 106-112 (2015).
[17] M. Wuttig and H. K. Birnbaum, "Self-Diffusion along Edge Dislocations in Nickel", Physical Review, Vol. 147, No. 2, pp. 495-505, (1966).
[18] W. Wycisk and M. Feller-Kniepmeier, "Quenching experiments in High Purity Ni", Journal of Nuclear Materials, Vol. 69-70, No. 1-2, pp. 616-619, (1978).